IRAQI Academic Scientific Journals

Tikrit Journal of Engineering Sciences (2020) 27 (2): 29-39.

ISSN: 1813-162X (Print) ; 2312-7589 (Online)

Tikrit Journal of Engineering Sciences

available online at: http://www.tj-es.com

TJES Tikrit Journal of Engineering Sciences

College of Engineering

Abdul Kareem KW, Fattah MY, Khaled ZS. Response of Different Machine Foundation Shapes Resting on Dry Sand to Dynamic Loading. *Tikrit Journal of Engineering Sciences* 2020; **27**(2): 29-39.

Khalid W. Abdul Kareem[1]*
Mohammed Y. Fattah[1]
Zeyad S. M. Khaled[2]

[1] Department of Civil Engineering, University of Technology, Baghdad, Iraq

[2] Department of Civil Engineering, Al-Nahrain University, Baghdad, Iraq

***Keywords*:**

Machine foundation, dynamic load, dry sand, amplitude displacement, strain, stress.

ARTICLE INFO

Article history:

Received	14 Oct. 2019
Accepted	20 July 2020
Available online	01 Sep. 2020

Response of Different Machine Foundation Shapes Resting on Dry Sand to Dynamic Loading

ABSTRACT

In this paper, the effect of footing shape resting on dry sand when subjected to machine dynamic loading is experimentally investigated. A laboratory set-up was prepared to simulate the case at different operating frequencies. Nine models were tested to examine the effects of the combinations of two parameters, including different frequencies of (0.5, 1, and 2 Hz) and different footing shapes (circular, square and rectangular). The tests were conducted under a load amplitude of (0.25 ton) using sand with medium and dense relative densities corresponding to (R.D. = 50% and 80%) having unit weights of (17.04 and 17.96 kN/m3) respectively. A shaft encoder and a vibration meter were used to measure the strain and amplitude displacement, while the stress in the soil at different depths was measured using flexible pressure sensors. It was found that the shape of footing has a considerable influence on the bearing capacity of the supporting soil under dynamic loading. For instance, the strain of dry sand under a circular footing was nearly (41%) higher, the amplitude displacement was nearly (17%) higher, and stress was nearly (12%) higher than square and rectangular footings, under the same conditions.

DOI: http://doi.org/10.25130/tjes.27.2.04

استجابة الأشكال المختلفة لأسس الماكينات المستندة على رمال جافة للتحميل الديناميكي

خالد وليد عبد الكريم/ قسم الهندسة المدنية/ الجامعة التكنلوجية , العراق
محمد يوسف فتاح/ قسم الهندسة المدنية/ الجامعة التكنلوجية, العراق
زياد سليمان محمد خالد/ قسم الهندسة المدنية/ جامعة النهرين, العراق

الخلاصة

في هذا البحث، تم التحري مختبرياً عن تأثير شكل الأسس المستندة على الرمل الجاف عند تعرضها للاحمال الديناميكية للماكنات. حيث تم تهيئة هيكل مختبري لمحاكاة الحالة بترددات تشغيل مختلفة. وتم اختبار تسعة نماذج لدراسة تأثير توليفات ذات عاملين يشملان ترددات مختلفة هي (0.5، و1، و2 هيرتز) وأشكال مختلفة للأسس هي (دائري، ومربع، ومستطيل). وأجريت الاختبارات تحت حمل بسعة (0.25 طن) باستخدام رمل ذي كثافتين متوسطة وعالية تبلغ (50٪ و80%) ووحدة وزن قدرها (17.04 و17.96 كيلونيوتن/م3) على التوالي. وقد استخدم مشفر العمود ومقياس الاهتزاز لقياس الانفعال وسعة الإزاحة، بينما تم قياس الاجهاد في التربة على أعماق مختلفة باستخدام مستشعرات ضغط مرنة. فوجد بأن لشكل الأساس تأثيراً واضحاً على قدرة تحمل التربة الداعمة له وهو تحت التحميل الديناميكي. وعلى سبيل المثال، كانت الاستجابة الديناميكية للرمال الجافة تحت الأسس الدائرية أعلى بنسبة (41٪) والهطول أعلى بنسبة (17%) والاجهادات أعلى بنسبة (12%) من الأسس المربعة والمستطيلة تحت نفس الشروط.

الكلمات الدالة: الة الأساس، حمل حركي، رمل جاف، سعة الموجة، الانفعال، الاجهاد.

* Corresponding Author: E-mail: Khalid_phar@yahoo.com Tel: +9647902450257

1. INTRODUCTION

The response of soil under dynamic loads is of great importance for the stability of structures because it is quite different from that of static loads. Many researchers stated that the stress-strain behavior of soil under dynamic loads is usually found to be hysteretic and nonlinear. Moreover, the response of

soil depends mainly on the level of stress that induces dynamic strains as well as the type of the soil, [1]. Therefore, the behavior of soil under dynamic loads can be considered as elasto-plastic to provide better estimations of displacement. In order to fulfill the aim of this research, which is to study the effect of the machine foundation shape on its response to dynamic loads generated by the machine itself, specific objectives were set. These objectives are to investigate the outcomes associated with different parameters, including; dynamic load (number of cycles and load frequency) on the strain amplitude displacement and stress in the soil at different depths. The investigation also includes explaining the influence of different shapes footing on the dynamic response.

Al-Homoud and Al-Maaitah [1] studied the effect of size and shape of footings on the load capacity behavior of sand foundation subjected to vertical vibration loads. It was concluded that the load capacity behavior in the base soil depends on the size and shape of the footing.

Boumekik et al. [2] presented laboratory tests to determine the dynamic stress of soil for three specific points of foundation-soil interface zone using a prototype of a vibrating foundation. The prototype proved to provide satisfying findings in simulating the behavior of superficial foundation under dynamic cyclic loading. A significant increase in the relative density of medium dense sand was observed because of particles' retightening at the central zone. As a result, the axial over-stresses are transferred to the edges due to primary confinement.

Nagaraj and Ullagaddi [3] investigated the influence of footing shape and size on sandy foundation settlement. The shape influence of circular, square, and rectangular footings of various areas was examined. The findings revealed that the bearing capacity and settlement of soil are also affected by the shape of footing as well as the size. Square footings, for instance, showed a higher degree of load carrying capacity and better load-settlement behavior.

Al-Shammary [4] conducted a numerical investigation to explore the dynamic reaction of stripped footing rested on saturated sand. A parametric investigation was carried out via PLAXIS 2D finite element software. The parametric investigation included evaluating different variables, namely; machine foundation breadth, dynamic loading amplitudes, dynamic loading frequency, soil mass damping, along with the foundation embedment. The outcomes indicated that the embedment provides a noticeable decrease in the dynamic reaction (excess pore water pressure and displacement) in various degrees for all types of soil used while keeping other parameters constant like damping ratio and soil density.

Al-Ameri [5] studied the response and behavior of the machine foundation resting on dry and saturated sand. A physical model was manufactured to investigate the soil and footing response to static and dynamic loads. Two sizes of rectangular steel footing of (100 x 200 x 12.5 mm) and (200 x 400 x 5.0 mm) were used. The dynamic loading frequencies used ranged from (500 rpm) to (3500 rpm). It was found that the maximum displacement capacity of the footing was halved when the size was doubled for both dry and saturated sand.

Fattah et al. [6] studied the effect of dynamic load frequency on the perpendicular displacement of the machine foundation using the restricted component investigation approach. It was found that the perpendicular displacement is reduced when the dynamic load frequency is increased.

Abd Al-Kareem et al. [7] studied the effect of footings embedment on amplitude displacement under the machine foundation. It was found that when the embedment depth is changed from zero (at the surface) to (0.5 B) and then to (B) the amplitude displacement is reduced by (21.5%) at depth (0.5 B) and (57%) at depth (B) on average.

2. MATERIAL USED

Footings of four shapes; circular, square, and two rectangular with different aspect ratios (length/width), made of (20 mm) thick steel plates were used, as shown in Fig. 1. The footings have the following shapes and dimensions:

1. Circular footing with a diameter of (150 mm).
2. Square footing of (132* 132 mm).
3. Rectangular footing of (150×100 mm).
4. Rectangular footing of (300*100 mm).

The sand used to carry out the tests was brought from Karbala province in Iraq, which is locally known as 'Al-Ikhaidur' sand. Its properties were obtained by performing standard tests on two different relative densities; medium and dense. Its physical characteristics were found to be categorized as poorly graded (SP) according to the Unified Soil Classification System (USCS). Table 1 summarizes the properties of the sand used, and Fig. 2. Shows its grain size distribution.

The experimental work was conducted using a steel cubical tank of (800×800×1000 mm) to hold the sand it was, made of (6 mm) thick plates of smooth faces.

The sand quantity used for each testing model was determined based on its relative density using equation (1).

$$(\mathbf{R.D.}) = \left(\frac{\mathbf{\Upsilon d(max)}}{\mathbf{\Upsilon d}}\right)\left(\frac{\mathbf{\Upsilon d - \Upsilon d(min)}}{\mathbf{\Upsilon d(max) - \Upsilon d(min)}}\right) \quad \text{.... (1)}$$

Where:

Υd_{max}: is the dry unit weight,

Υd_{max}: is the maximum dry unit weight, and

Υd_{min}: is the minimum dry unit weight.

In order to ensure uniformity throughout the depth of the model, (100 mm) thick layers of sand were placed layer by layer and compacted manually by a small plate to the marked levels. Each layer placed was leveled as to assure that the foundation is sitting on a horizontal surface.

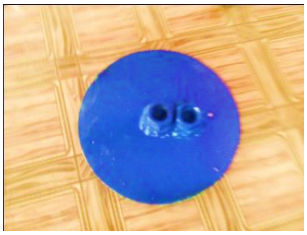
Circular


Square


Rectangular (L/B=1.33)


Rectangular (L/B=3)

Fig. 1. Types of footings used

Table 1
Properties of sand used

Index properties	Value	Specifications
Specific gravity Gs	2.66	ASTM D 854[8]
Coefficient of uniformity C_u	3.91	ASTM D 422[9]
Coefficient of curvature C_c	0.77	ASTM D 422 [9]
Soil classification *USCS*	SP	
Maximum dry unit weight (kN/m³)	19.0	ASTM D 4253 [10]
Minimum dry unit weight (kN/m³)	16.0	ASTM D 4254 [10]
Maximum void ratio	0.66	……
Minimum void ratio	0.4	……
Angle of internal friction ϕ at *R.D* =50%	39.5°	ASTM 3080 [11]
Angle of internal friction ϕ at *R.D* =80%	42°	ASTM 3080 [11]

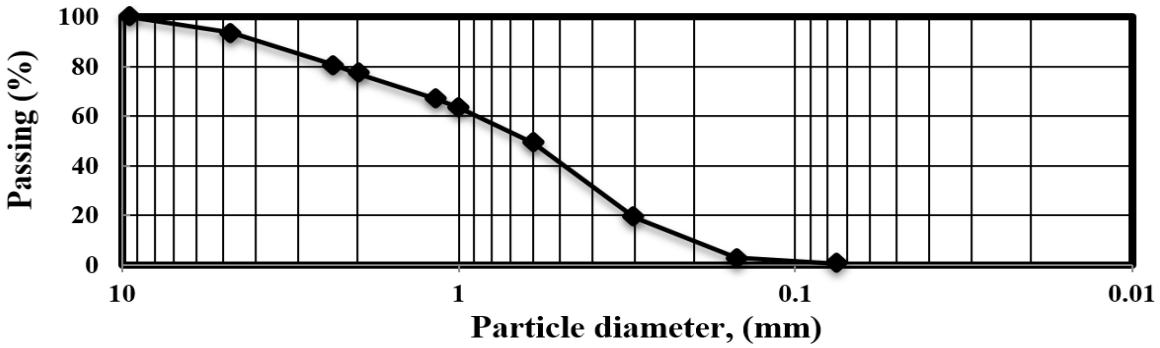

Fig .2. Grain size distribution curve for sand used.

3. MODEL SET-UP

3.1 Loading system

In order to simulate the real life situation, a proper model set-up was prepared and equipped with relevant accessories to form the loading system needed, as shown in Fig. 3. The model set-up consists of a steel container, loading frame, electro-hydraulic jack, footing plates, settlement measuring device, and data logging and acquisition system.

3.2 Vibration meter

A vibration meter was mounted to measure movements in three directions (x, y, and z). The vibration device included an ADXL345 type accelerometer, which is a 3-axis small power device with sign condition electrical energy output, as shown in Fig. 4.

3.3 Flexible force sensor

Ultra-thin flexible tactile flexi force pressure sensors of (1500 kPa) capacity were utilized to measure stresses in the sand at two depths (B and 2B), where (B) is the width of footing as shown in Fig. 5. The sensors' dimensions were (14×25.4 mm) and (0.203 mm) thick with sensing area diameter of (9.53 mm). Two load pressure senores were used in order to investigate the change in stresses at different depths because the distribution of stresses in the soil under dynamic load is often deep.

4. RESULTS AND DISCUSSIONS

The tests were carried out using sand with two relative densities of (50% and 80%), load amplitude of (0.25 ton) frequencies of (0.5, 1 and 2 Hz) and for shapes of footings (circular, square and rectangular with two aspect ratios (L/B = 1.33 and 3). The results of all tests are listed in the following tables; nevertheless, the results of dense sand are not shown in figures to avoid redundancy, for they show the same trend but with higher values. Again, the results of the rectangular footing of (L/B=3) are not shown in figures for the same reason but with much lower values.

4.1 Effect of the footing shape on the strain

The measured strain is presented by (S_N/H) where (S_N) is the settlement of the footing at any number of cycles, and (H) is the thickness of the sand layer in the container. Table 2 and Figures (6 to 9) show the readings of strain versus the number of load cycles after (1000) cycles for different shapes of footing under different frequencies with the same load amplitude. The strain was (33%) higher when the rectangular footing of (L/B= 1.33) was replaced by the square footing and (19%) higher when replaced by the circular footing. This behavior is attributed to the increase in the bearing pressure intensity applied to the soil when the contact area of the footing decreases. Furthermore, the static bearing capacity of the rectangular footing is higher than that of the square, as given in equations (2-4) [12]. This agrees with the findings by [2].

$$q_{ult} = 1.3\ c\ N_c + q\ N_q + 0.3\ \gamma\ B\ N_\gamma$$

(for circular footing) **...(2)**

$$q_{ult} = 1.3\ c\ N_c + q\ N_q + 0.4\ \gamma\ B\ N_\gamma$$

(for square footing) **... (3)**

$$q_{ult} = 1.3\ \frac{B}{L}\ c\ N_c + q\ N_q + \left(1 - 0.2\frac{B}{L}\right) 0.5\ \gamma B\ N_\gamma$$

(for rectangular footing) **... (4)**

Where: Nc, Nq, N γ are the bearing capacity factors.

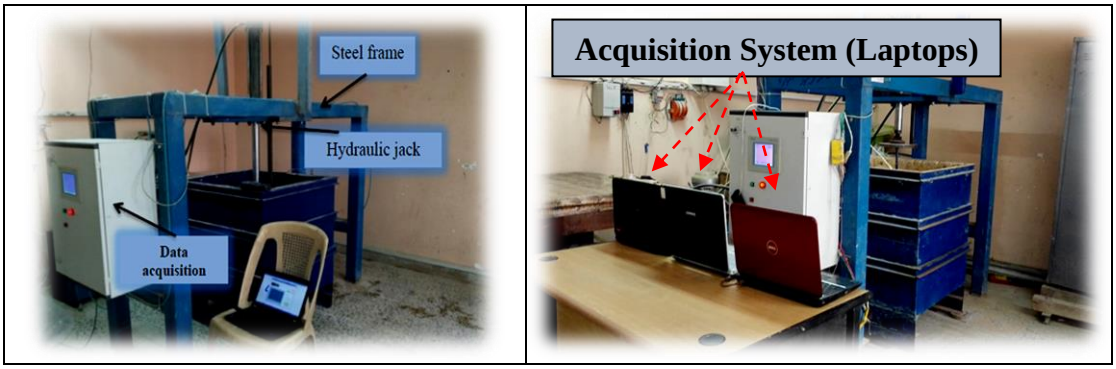

Fig.3. The model set-up and accessories

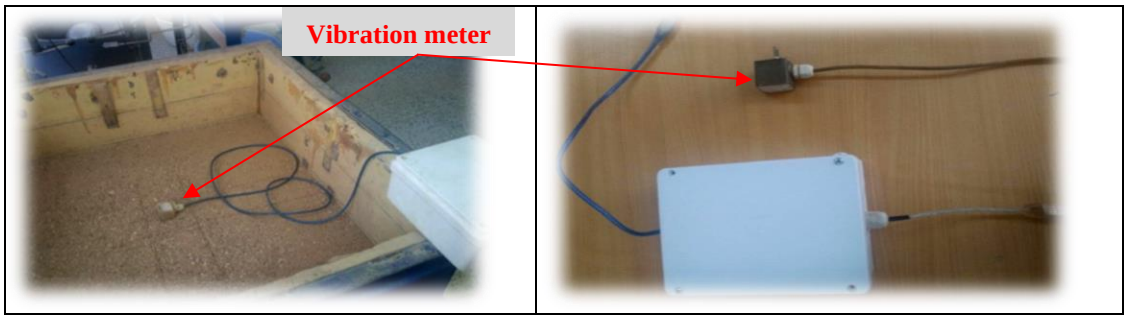

Fig.4 . Vibration meter

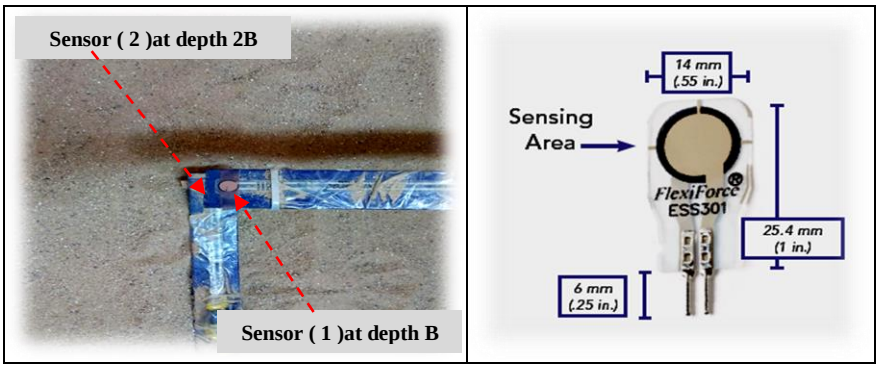

Fig. 5. Tactile pressure sensors

Table 2

Strain after (1000) cycles at different frequencies under load amplitude of (0.25 ton)

Footing shape	0.5 Hz		1 Hz		2 Hz	
	50%	80%	50%	80%	50%	80%
Circular	0.017	0.009	0.013	0.008	0.008	0.006
Square	0.015	0.006	0.008	0.006	0.007	0.005
Rectangular (L/B= 1.33)	0.014	0.006	0.007	0.005	0.006	0.004
Rectangular (L/B= 3)	0.005	0.003	0.004	0.003	0.002	0.001

On the other hand, the strain had increased when the loading frequency was decreased for all shapes of footings. It had increased by (41%) and (68%) when the frequency was decreased from (2 to 1 Hz) and (1 to 0.5 Hz), respectively. This is because the low frequency of loading provides enough time for soil densification, and so it leads to increased strain. This agrees with the findings by [7].

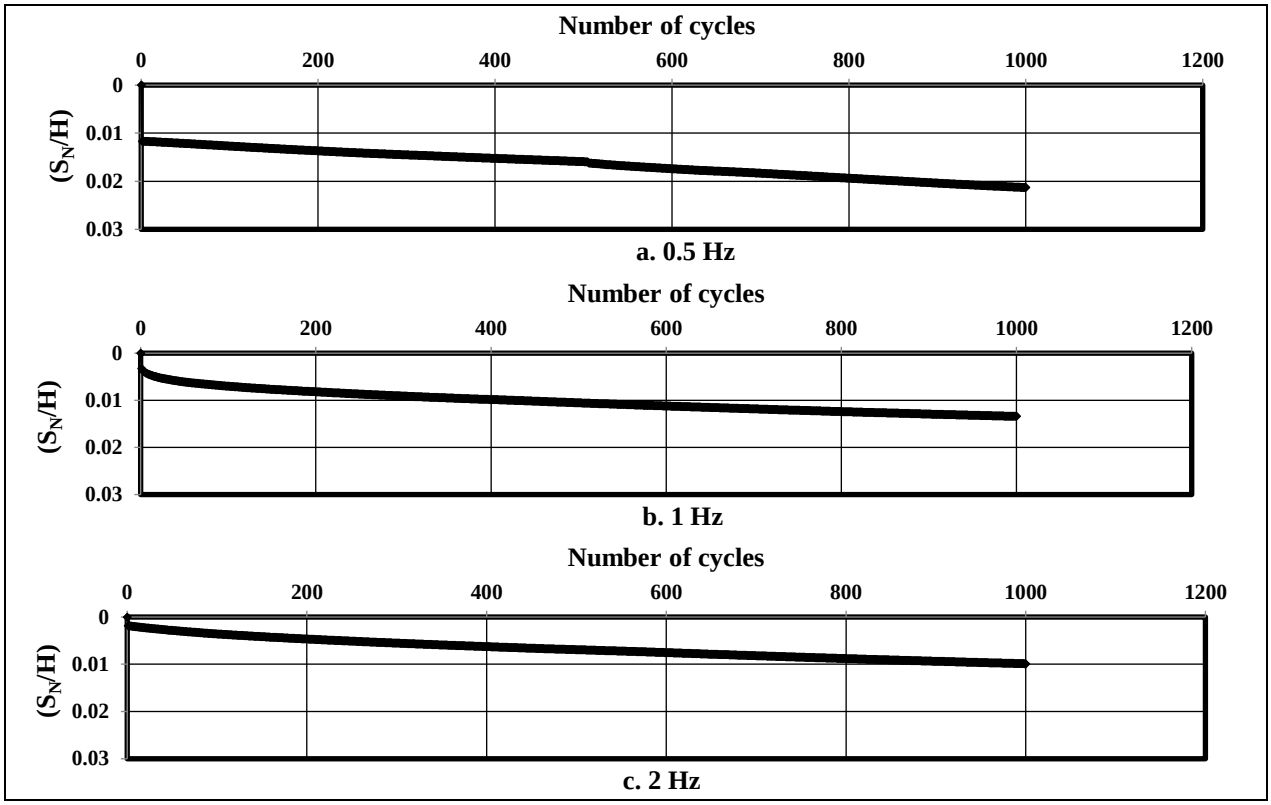

Figure 6: Number of cycles vs. strain of circular footing under load amplitude of (0.25 ton)

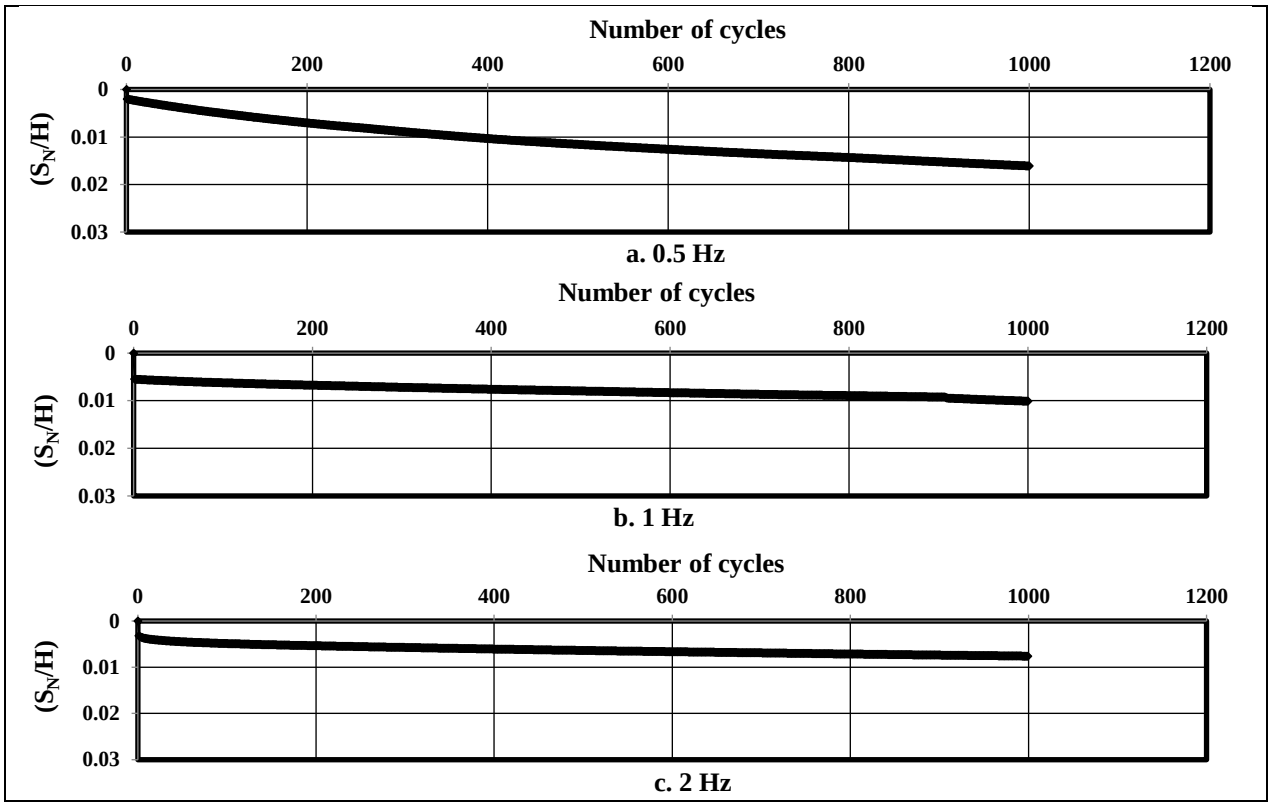

Figure 8: Number of cycles vs. strain of square footing under load amplitude of (0.25 ton)

4.2 Effect of the footing shape on amplitude displacement

As can be seen in Table 3, the maximum amplitude displacement of the rectangular footing of (L/B=1.33) is (40%) lower than that of circular footing.

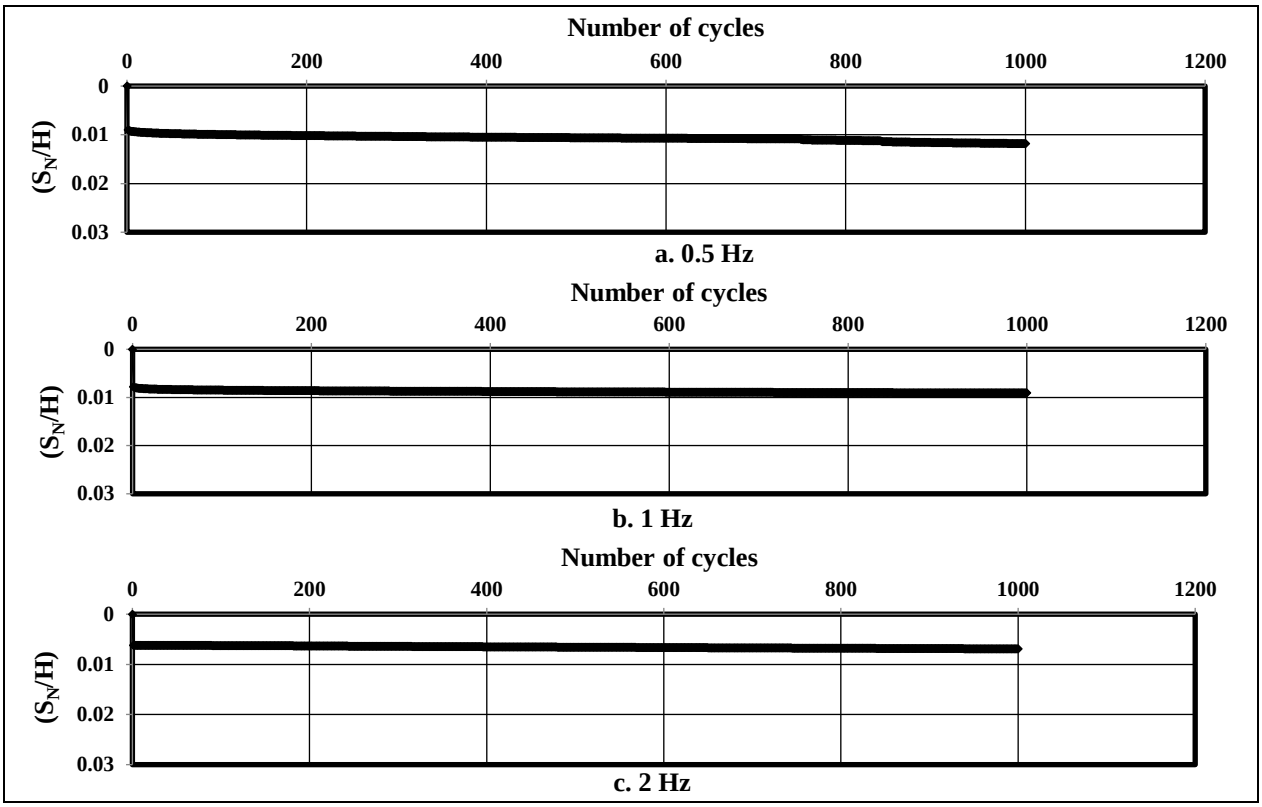

Figure 9: Number of cycles vs. strain of rectangular footing under load amplitude of (0.25 ton)

This reduction is attributed to the large contact area of the rectangular footing, which leads to lower stress. The relationship of the amplitude displacement vs. the number of cycles was established. Figures (10 to 12) shows the results of measured amplitude displacement for the same aforementioned tests. It can be noticed that the trend of all results is the same. The results agree with the findings by [13] and [14].

Table 3

Absolute amplitude displacement (mm) after (1000) cycles at different frequencies under load amplitude of (0.25 ton)

Footing shape	0.5 Hz		1 Hz		2 Hz	
	50%	80%	50%	80%	50%	80%
Circular	2.66	1.72	2.16	1.53	1.98	1.34
Square	2.39	1.65	1.94	1.39	1.65	1.23
Rectangular (L/B= 1.33)	2.24	1.32	1.77	1.27	1.70	1.12
Rectangular (L/B= 3)	1.53	1.25	1.41	1.13	1.24	1.05

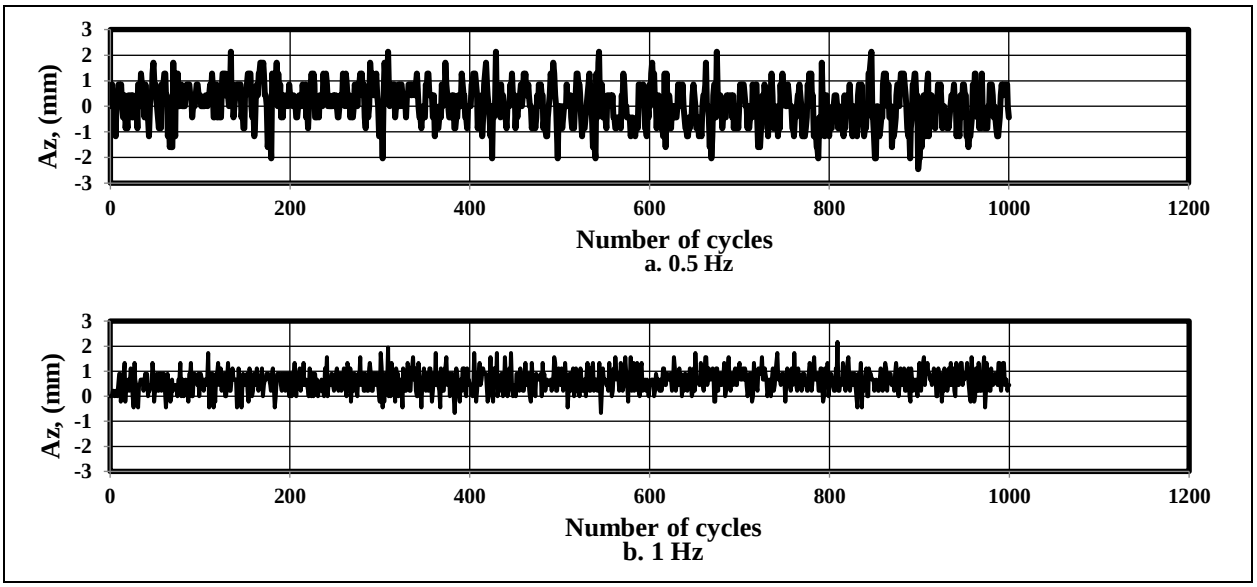

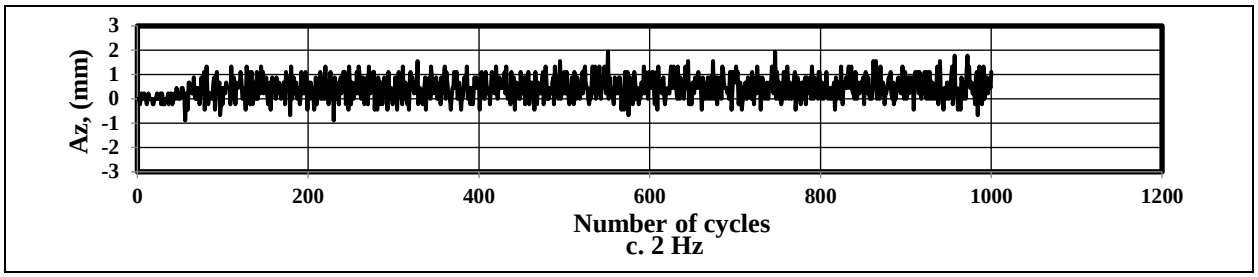

Fig. 10. Number of cycles vs. amplitude displacement of circular footing under load amplitude of (0.25 ton)

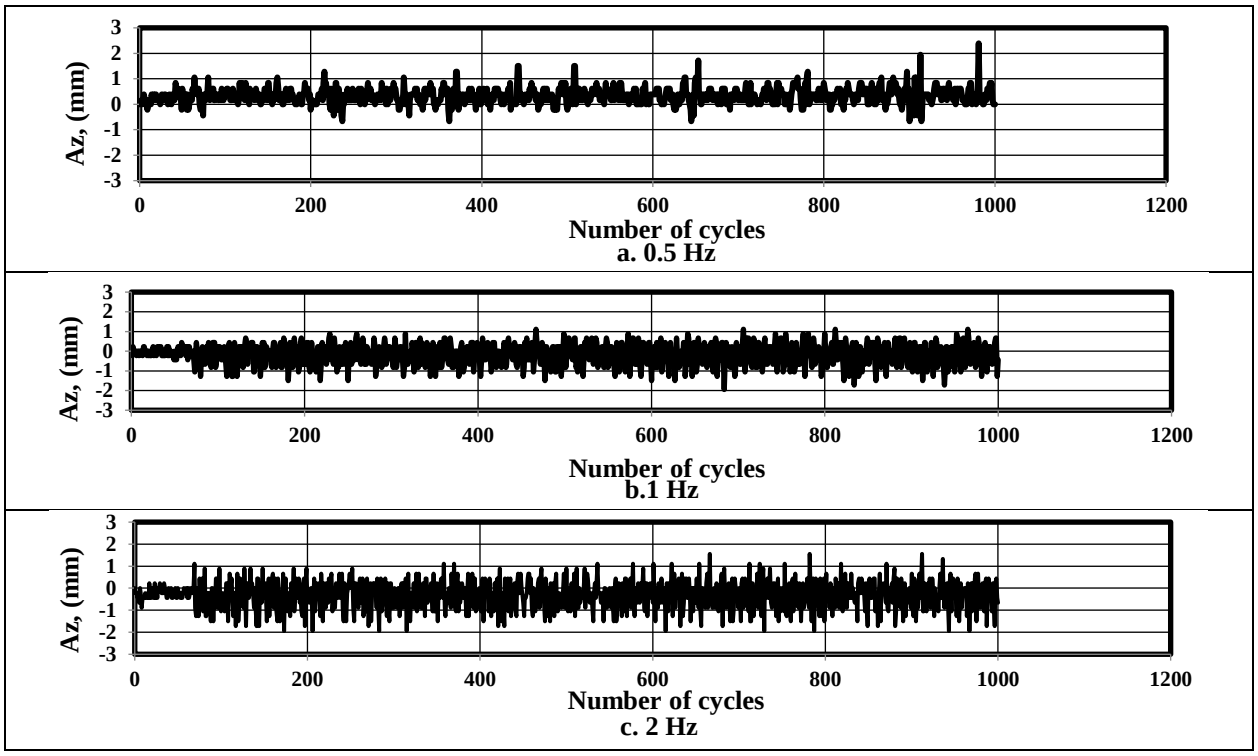

Figure 11: Number of cycles vs. amplitude displacement of a square under load amplitude of (0.25 ton)

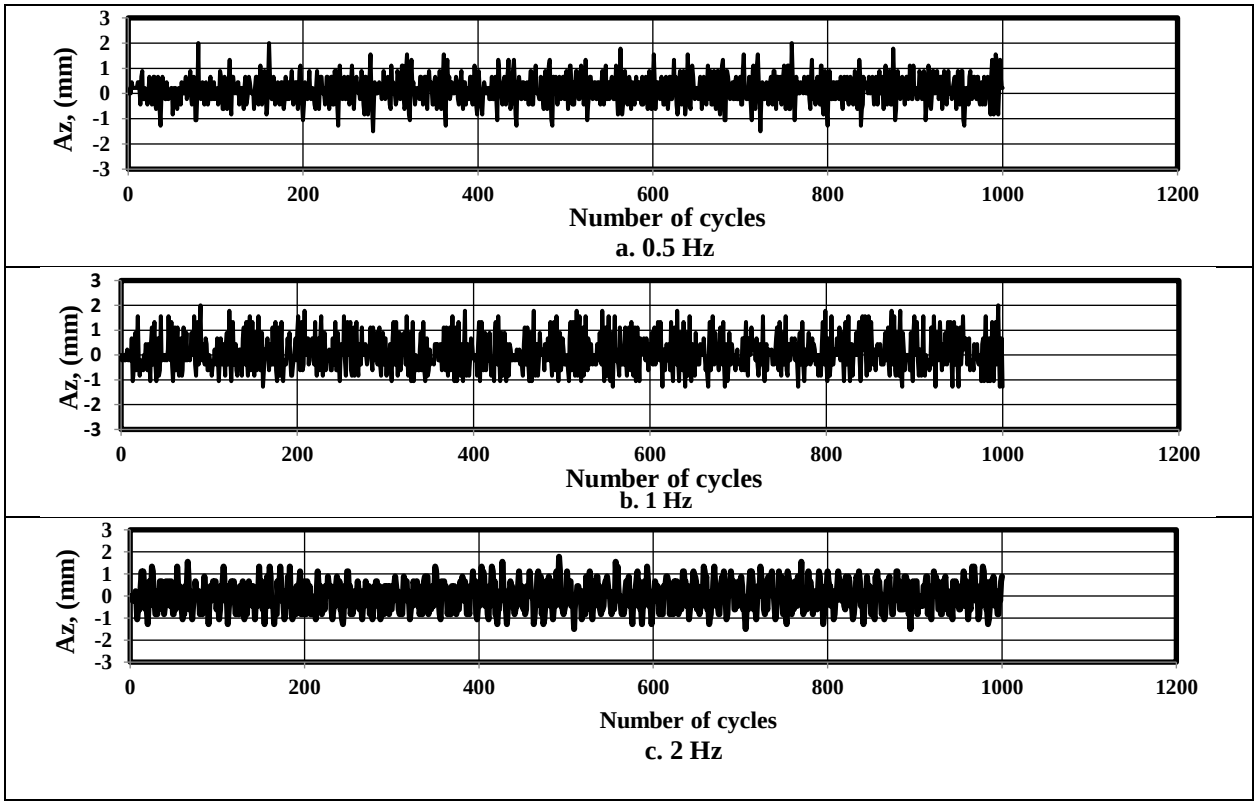

Fig.12 . Number of cycles vs. amplitude displacement of a rectangular footing under load amplitude of (0.25 ton)

4.3 Effect of the footing shape on stress

Stresses inside the soil were measured using a new technique in which two flexi force pressure sensors were used. These sensors were positioned in the proper locations to measure the stresses conveyed to the soil layer via the applied dynamic load at depths (B and 2B). Figures (13 to 18) show the relationship of total dynamic stress ($T\sigma_{dyn}$) versus the number of cycles for the two flex force pressure sensors. It can be noticed that almost in all the tests, the stresses at both depths had started from a certain level and remain for a period, then increased rapidly until a maximum magnitude and then decreased in a cyclic manner of increasing and decreasing. This happens more likely when using flexi force pressure sensors that are directly located under the loading effect at both depths because the interlocking of sand particles affects their confinement. Hence the interlocking is low at the beginning of the tests, and then it increases with time because of the reorientation of sand particles. It can be noticed for all depths, that there is an increase in the maximum average stress with decreased operating frequency.

For instance, when the sensor was located at depth (B) in the sand, and the frequency was decreased from (2 to 1 Hz), the dynamic stresses increased (7.2%). When the frequency was decreased from (1 to 0.5 Hz), the dynamic stresses increased (15.27%). These dynamic stresses became (8.11%) and (12.52%) when the sensor is located at depth (2B), respectively.

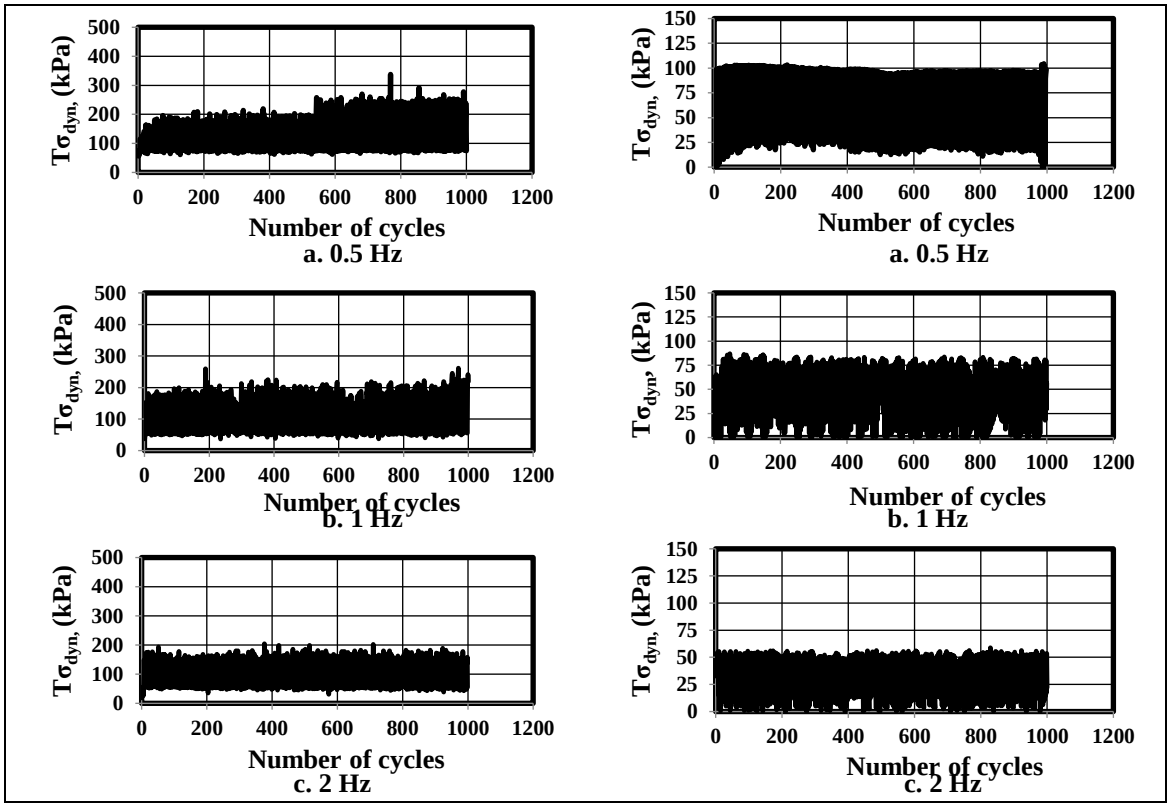

Fig. 13. Number of cycles vs. total dynamic stress for circular footing at depth B under load (0.25 ton) on the sand having R.D. = 50%.

Fig. 14. Number of cycles vs. total dynamic stress for circular footing at depth 2B under load (0.25 ton) on the sand having R.D. = 50%.

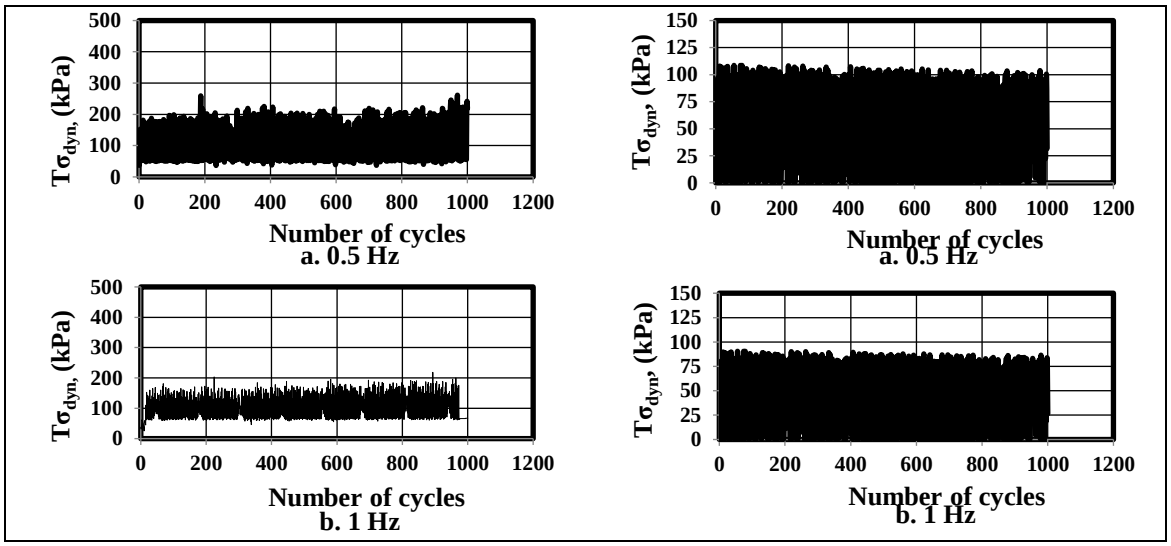

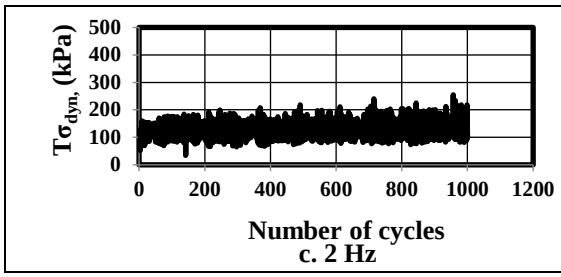

Fig.15. Number of cycles vs. total dynamic stress for square footing at depth B under load (0.25 ton) on the sand having R.D. = 50%.

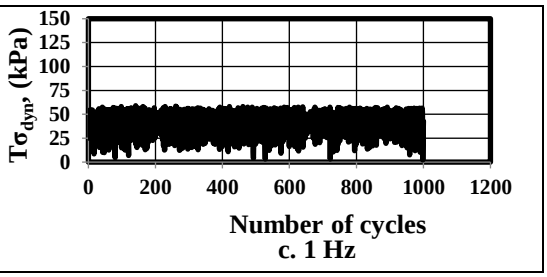

Fig. 16. of cycles vs. total dynamic stress for square footing at depth 2B under load (0.25 ton) on the sand having R.D. = 50%.

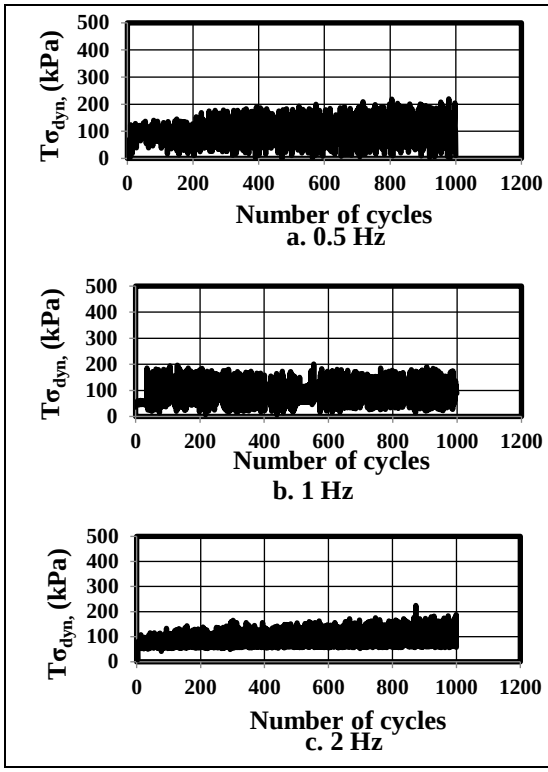

Fig. 17. Number of cycles vs. total dynamic stress for rectangular footing at depth B under load (0.25 ton) on the sand having R.D. = 50%.

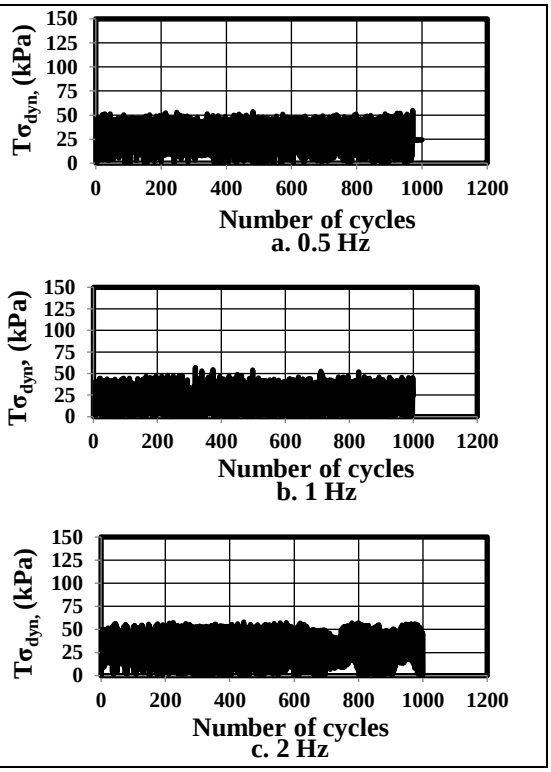

Fig. 18. Number of cycles vs. total dynamic stress for rectangular footing at depth 2B under load (0.25 ton) on the sand having R.D. = 50%.

Tables (4) and (5) list maximum average dynamic stresses measured at depths (B and 2B) for medium and dense sand. In general, the measured stresses seem to indicate higher values at both depths as compared to the classical method for obtaining the stress increment under the footing in which stresses are calculated according to the theory of elasticity or (2:1) method. This behavior is attributed to the combination of generated dynamic stresses and the initial static stress in the soil.

Table 4: Maximum average dynamic stress (kPa) after (1000) cycles at different depths below surface footing resting on medium density sand of (R.D. = 50%)

Circular footing - Load amplitude = 0.25 ton					
f_o= 0.5 Hz		**f_o= 1 Hz**		**f_o= 2 Hz**	
B	**2B**	**B**	**2B**	**B**	**2B**
108.41	48.50	91.34	39.9	84.62	36.86
Square footing – Load amplitude = 0.25 ton					
f_o= 0.5 Hz		**f_o= 1 Hz**		**f_o= 2 Hz**	
B	**D_s= 2B**	**B**	**2B**	**B**	**2B**
98.87	42.98	85.81	37.11	81.62	34.97
Rectangular footing (L/B= 1.33) – Load amplitude = 0.25 ton					
f_o= 0.5 Hz		**f_o= 1 Hz**		**f_o= 2 Hz**	
B	**2B**	**B**	**2B**	**B**	**2B**
90.97	33.56	81.35	30.54	75.86	28.98
Rectangular footing (L/B= 3) – Load amplitude = 0.25 ton					
f_o= 0.5 Hz		**f_o= 1 Hz**		**f_o= 2 Hz**	
B	**2B**	**B**	**2B**	**B**	**2B**
81.87	31.49	74.48	30.74	65.27	27.73

Table 5: Maximum average dynamic stress (kPa) after (1000) cycles at different depths below surface footing resting on dense density sand of (R.D. = 80%)

Circular footing - Load amplitude = 0.25 ton					
f_o= 0.5 Hz		**f_o= 1 Hz**		**f_o= 2 Hz**	
B	**2B**	**B**	**2B**	**B**	**2B**
87.67	40.77	79.81	33.75	72.27	31.62
Square footing – Load amplitude = 0.25 ton					
f_o= 0.5 Hz		**f_o= 1 Hz**		**f_o= 2 Hz**	
B	**D_s= 2B**	**B**	**2B**	**B**	**2B**
84.53	35.45	71.92	32.3	65.64	30.62
Rectangular footing (L/B= 1.33) – Load amplitude = 0.25 ton					
f_o= 0.5 Hz		**f_o= 1 Hz**		**f_o= 2 Hz**	
B	**2B**	**B**	**2B**	**B**	**2B**
75.95	27.72	68.59	25.31	62.07	23.83
Rectangular footing (L/B= 3) – Load amplitude = 0.25 ton					
f_o= 0.5 Hz		**f_o= 1 Hz**		**f_o= 2 Hz**	
B	**2B**	**B**	**2B**	**B**	**2B**
66.61	26.19	60.59	24.57	53.36	22.98

5. CONCLUSIONS

Based on the results of this research, the following conclusions can be drawn:

1. The bearing capacity of the machine foundation resting on sandy soil and subjected to dynamic loading generated from the machine is affected by the shape of footing in addition to its area. It has been noticed to be higher for circular footing than a square or rectangular one.
2. The curves of cyclic strain were found to have a similar trend, in which there is a sharp increase in the rate of strain up to (500) cycles, and then a gradual increase is sustained till it vanishes at (700 - 1000) cycles depending on the applied frequency.
3. The amplitude displacement had decreased with the increased operating frequency and area of the footing.
4. The stress within the soil medium can be measured with high confidence using flexible pressure sensors. Nevertheless, it should be noticed that soil stress increments resulting from dynamic loading applied to the foundation reduce with depth. For instance, stress at depth (B) is up to (58.36%) higher than that at depth (2B).
5. Rectangular footing has shown lower dynamic response behavior compared to circular and square footings.

REFERENCES

[1] Al-Homoud, A. S., and Al-Maaitah, O. N. An Experimental Investigation of Vertical Vibration of Model Footings on Sand, *Soil Dynamics and Earthquake Engineering*, 1996; 15(**7**): 431-445.

[2] Boumekik, A., Belhadj-Mostefa, S. and Meribout, F. Experimental Analysis of the Dynamic Stress Distribution at the Soil Foundation Interface, *Asian Journal of Civil Engineering*, Building and Housing, 2010; 11(**5**): 575-583.

[3] Nagaraj, T. K., and Ullagaddi, P. B. Experimental Study on Load Settlement Behavior of Sand Foundations", *Indian Geotechnical Conference*, Bombay, GEO trends, December 16-18, 2010, IGS Mumbai Chapter and IIT Bombay, pp. 807-808.

[4] Al-Shammary W. T. S. Numerical Analysis of Machine Foundation on Saturated Sandy Soil". M.Sc. Thesis, Building and Construction Engineering Department, University of Technology, Iraq, 2013.

[5] Al-Ameri, A. F. I. Transient and Steady State Response Analysis of Soil Foundation System Acted upon by Vibration". Ph.D. Thesis, Civil Engineering Department, University of Baghdad, Iraq, 2014.

[6] Fattah, M. Y., Al-Mosawi, M. J., and Al-Ameri, A. F. I. Dynamic Response of Saturated Soil – Foundation System Acted upon by Vibration. *Journal of Earthquake Engineering*, 2017; 21: 1158–1185.

[7] Abdul Kareem, K. W., Fattah, M. Y. and Khaled, Z. S. M. Effect of Embedment Depth for Circular Footing on the Amplitude of Displacement under Dynamic Load. *3rd International Conference on Engineering Sciences.* 2019, Kerbala, Iraq, IOP Conf. Series: Materials Science and Engineering 671.

[8] American Society of Testing and Materials, (ASTM). Standard Test Method for Specific Gravity. ASTM D 854, West Conshohocken, Pennsylvania, USA, 2010.

[9] American Society of Testing and Materials (ASTM). Standard Test Method for Particle Size Analysis of Soils. ASTM D 422, West Conshohocken, Pennsylvania, USA, 2010.

[10] American Society of Testing and Materials (ASTM). Standard Test Method for Maximum and Minimum Index Density and Unit Weight of Soils Using a Vibratory Table. ASTM D 4253-4254, West Conshohocken, Pennsylvania, USA, 2010.

[11] American Society of Testing and Materials (ASTM). Standard Test Method for Direct Shear Test of Soils Under Consolidated

Drained Conditions. ASTM D 3080, West Conshohocken, Pennsylvania, USA, 2010.

[12] Das B. M. and Ramana G. V., Principles of Soil Dynamics". (2nd) Edition, Cengage Learnung, Stanford, USA, 2011.

[13] Al-Obaidi AA, Al-Mukhtar MT, Al-Dikhil OM, Hannona SQ .Comparative Study between Silica Fume and Nano Silica Fume in Improving the Shear Strength and Collapsibility of Highly Gypseous Soil. *Tikrit Journal of Engineering Sciences* 2020; 27(1): 72- 78.

[14] Fattah, M. Y., Al-Mosawi, M. J., and Al-Ameri, A. F. I. Stresses and Pore Water Pressure Induced by Machine Foundation on Saturated Sand. Ocean Engineering, 2016; 146: pp. 268–281.